

## **Influence of Alkali Metal Oxides and Alkaline Earth Metal Oxides on the Mitigation of Stress Corrosion Cracking in CANDU Fuel Sheathing**

**\*J. Metzler, G.A. Ferrier, M. Farahani, P.K. Chan, and E.C. Corcoran**

Royal Military College of Canada, Kingston, Ontario, Canada

[\\*\(Joseph.Metzler@rmc.ca\)](mailto:Joseph.Metzler@rmc.ca)

*Note: A condensed version of this paper has been submitted to the parallel 39<sup>th</sup> CNS/CNA Student Conference to be presented as a poster.*

### **Abstract**

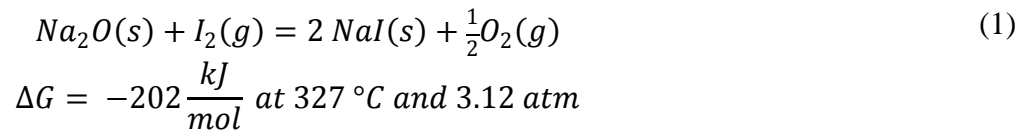
This work investigates strategies to mitigate stress corrosion cracking (SCC) in Zircaloy-4 sheathing materials. The CANLUB coatings currently used in CANDU reactors contain both alkali metal and alkaline earth metal impurities, which can exist as oxides (*e.g.*, Na<sub>2</sub>O and CaO). It is believed that when the corrosive fission product iodine reacts with these oxides, the iodine can be sequestered through the formation of an iodide (*e.g.*, NaI and CaI<sub>2</sub>). The subsequent O<sub>2</sub> release may repair cracks in the protective ZrO<sub>2</sub> layer on the sheathing, shielding the Zircaloy-4 sheathing from further corrosive fission product attack. For this investigation, O<sub>2</sub> gas, Na<sub>2</sub>O, and CaO were separately introduced into an environment wherein slotted Zircaloy-4 rings endure mechanical stresses in iodine vapour at high temperatures. Controlled additions of O<sub>2</sub> gas created a slight reduction in the corrosive attack on Zircaloy-4 sheathing, while the inclusion of Na<sub>2</sub>O and CaO lead to greater reductions.

### **1. Introduction**

Stress corrosion cracking (SCC) is a process that can initiate defects in the Zircaloy-4 (Zr-4) fuel sheathing used in CANDU<sup>®</sup> nuclear reactors. Although the current defect rate is very low in CANDU reactor operation, a defect can cause fuel oxidation as well as the transport of harmful, radioactive fission products through the sheath into the primary heat transport system. There are three criteria that must be met for SCC to occur: i) a susceptible material; ii) a *sufficient strain* must be reached; and iii) the surrounding environment must be sufficiently *hot* and *corrosive* [1]. In CANDU reactors, thermal and radiation-induced swelling of uranium dioxide fuel pellets induces circumferential sheath strains (0.8-1.3% [2]) that exceed the strain levels (0.1-0.5% [3]) required for SCC of Zr-4 sheathing. The sheath experiences these strain levels at elevated temperatures (> 300°C) while the presence of the fission product iodine is present in sufficient quantities (> 1-5 mg cm<sup>-3</sup>) [4] to create the required corrosive environment. Although current SCC mitigation strategies are effective in limiting sheath failure rates (~0.01%), SCC contributes the largest portion of these failures (35%) when compared to other failure mechanisms [5]. Thusly, alternative SCC mitigation strategies are being investigated as improving SCC mitigation justifies significant consideration in the effort to reach more advanced fuel cycles in CANDU reactors (*e.g.*, higher burnups or load-following regimes).

Part of the original SCC mitigation strategy developed in 1972 was CANLUB, a graphite coating applied to the Zr-4 fuel sheathing. It was predicted that CANLUB would provide mechanical lubrication in order to prevent SCC failures by lowering the stresses induced in the sheath [6]. While the introduction of CANLUB and other SCC mitigation strategies did lead to a reduction of fuel failures [4], evidence indicates that the surrounding moisture levels do not allow the coating to provide sufficient lubrication to lead to the observed decrease in SCC failures [7]. Also, CANLUB has been

shown to be an ineffective physical barrier [8]. The success of CANLUB is now believed to arise mainly from the coating's ability to sequester iodine in chemical reactions, thus preventing the corrosive element from interacting with the fuel sheath. For example, Chan *et al.* demonstrated that the corrosive element iodine ( $I_2$ ), which is produced as a fission product in CANDU reactors, can form  $Zr_xI_yC$  compounds near the CANLUB-Zircaloy interface, effectively sequestering the  $I_2$  [6]. Another potential iodine-sequestering reaction involves the reaction of iodine and alkali metal oxide impurities within the CANLUB coating, as suggested by Lewis *et al.* [3]. For example, the alkali metal oxide,  $Na_2O$ , has the potential to successfully sequester corrosive iodine while providing the added benefit of releasing oxygen that could possibly repair the protective oxide layer on the sheath (Equation 1).



The negative  $\Delta G$  for this reaction indicates that the products are favoured. The pressure level in Equation 1 was used to replicate the experimental conditions used in this work (Section 2), determined through the use of ideal gas laws to find the pressure created in the ampoule through the sublimation of  $I_2$  at high temperatures. The products of Equation 1 indicate that iodine is sequestered as an iodide compound ( $NaI(s)$ ) and that oxygen gas ( $O_2(g)$ ) is released. A similar reaction may be seen using alkaline earth metals, which were also considered in this investigation.

Inductively coupled plasma mass spectrometry has been used to determine that sodium (Na) and calcium (Ca) are alkali (and alkaline earth) metal impurities found in significant quantities in CANLUB (*e.g.*,  $220 \pm 10 \text{ ppm}_{Na}$  and  $210 \pm 30 \text{ ppm}_{Ca}$ ) [9]. Consequently, in this work, these elements were incorporated as oxides into SCC experiments to determine their ability to reduce the iodine-induced corrosion of Zr-4 sheathing. Similarly, in other SCC experiments,  $O_2$  gas was incorporated directly to evaluate the protective capabilities of oxygen when the oxide impurities were excluded. These experiments are built upon the work of Wood [10] and the results are compared to the baseline dataset collected by Metzler *et al.* [11].

## 2. Experimental Procedure

In the following experiments slotted rings cut from Zr-4 sheathing were exposed to hot, stressful, and corrosive environments in order to evaluate their susceptibility to SCC. A Buehler Isomet 1000 precision saw equipped with a diamond blade (151 mm diameter and 0.6 mm thickness) was used to cut Zr-4 tubing (diameter =  $13.10 \text{ mm} \pm 0.05 \text{ mm}$ ) into slotted rings having a fixed width ( $5.00 \text{ mm} \pm 0.05 \text{ mm}$ ) and slot opening ( $2.30 \text{ mm} \pm 0.08 \text{ mm}$ ). The slotted rings were sequentially polished using 320- and 600-grit silicon carbide paper to create smooth surfaces and edges.

In a typical experiment, eight slotted rings (stressed on two Zr-4 wedges) were placed in a cylindrical Pyrex ampoule, along with a small glass vial containing a known amount of iodine (Figure 1). The iodine vial featured a goose-neck and contained a trace amount of argon. This made it possible to break open the iodine vial with gentle agitation at the desired point in the experiment. Select experiments (Table 1) featured  $Na_2O$  or CaO powder additions (Aldrich Chemistry, Oakville), or  $O_2$  additions (Section 2.1).



**Figure 1: Sealed capsule with ring-wedge assembly and iodine vial.**

**Table 1: Summary of experiments performed. Experiments were performed on wedge sizes ranging from 6-12 mm and all tests were performed with  $1530 \pm 10$  mg of  $I_2$ .**

Temperature / (°C)	O <sub>2</sub> Gas / (Torr)	Na <sub>2</sub> O / (g)	CaO / (g)	Number of Samples (N)
300 ± 10	0	0	0	24
375 ± 10	0	0	0	8
300 ± 10	6.0 ± 0.5	0	0	16
375 ± 10	6.0 ± 0.5	0	0	16
300 ± 10	12 ± 1	0	0	8
375 ± 10	12 ± 1	0	0	10
300 ± 10	54 ± 2	0	0	16
375 ± 10	54 ± 2	0	0	18
300 ± 10	0	0.68 ± 0.02	0	16
300 ± 10	0	0.84 ± 0.02	0	8
300 ± 10	0	0	0.08 ± 0.02	24
300 ± 10	0	0	0.17 ± 0.02	24
300 ± 10	0	0	0.25 ± 0.02	24
300 ± 10	0	0	0.34 ± 0.02	24

The loaded ampoule was attached to a vacuum system designed to remove moisture and air from the ampoule. Initially, for approximately 5-10 minutes, a rotary pump (Alcatel) removed the bulk amount of oxygen from the ampoule by lowering the vacuum pressure from atmospheric pressure (760 Torr) to 0.05 Torr. Having a low oxygen pressure enabled a turbomolecular pump (Varian Turbo – V70D Macro Torr) to subsequently lower the vacuum pressure to approximately 7-30 μTorr over the course of 18-24 h. Once the final vacuum level was achieved, the ampoule was flame-sealed. At this point, the iodine vial was broken to release iodine into the sealed ampoule just before the ampoule was placed into a tube furnace for five days at 300 or 375°C.

## 2.1 O<sub>2</sub> Additions

In some experiments (Table 1), the ampoule was vacuumed to 7-30 μTorr and then re-filled with O<sub>2</sub> gas to specified pressure levels before flame-sealing the ampoule. These experiments were intended to determine whether O<sub>2</sub> gas mitigates SCC, possibly by repairing cracks in the protective oxide layer. In addition, these experiments attempt to confirm previous results found by this research group [12]. The levels of oxygen utilized were 1, 2, and 9 μmol O<sub>2</sub> cm<sup>-3</sup> Zr-4, which correspond to oxygen partial pressures of 6, 12, and 54 Torr, respectively.

The process of delivering O<sub>2</sub> gas to an ampoule began by connecting the ampoule to a pressurized gas tank (Air Liquide, Montreal) containing 99.999% pure O<sub>2</sub> gas using a valve system (Figure 2) consisting of a three-way valve followed by two consecutive bleed valves. Placing two bleed valves in series allows for precise control of O<sub>2</sub> gas flow into the ampoule.

During the initial process of vacuuming the ampoule, both bleed valves were fully opened and the three-way valve was directed to open atmosphere, allowing the system to be placed under vacuum all the way up to the three-way valve. Once the system reached 7-30 μTorr, O<sub>2</sub> gas was used to flush the piping between the tank and the three-way valve, which was still open to the atmosphere (Figure 2A). At this point, the vacuum pump was turned off, the bleed valves were both closed, and the three-way valve was dialled to direct the flow of oxygen toward the ampoule and closed bleed valves. The bleed valves were opened slightly to allow a controlled flow of O<sub>2</sub> gas into the valve system and ampoule (Figure 2B). A pressure gauge, downstream of the bleed valves, was carefully monitored until the pressure reached the desired level. After which, the O<sub>2</sub> gas supply was turned off and the ampoule was promptly flame-sealed, detached, and placed in a tube furnace for five days at 300 or 375 °C.

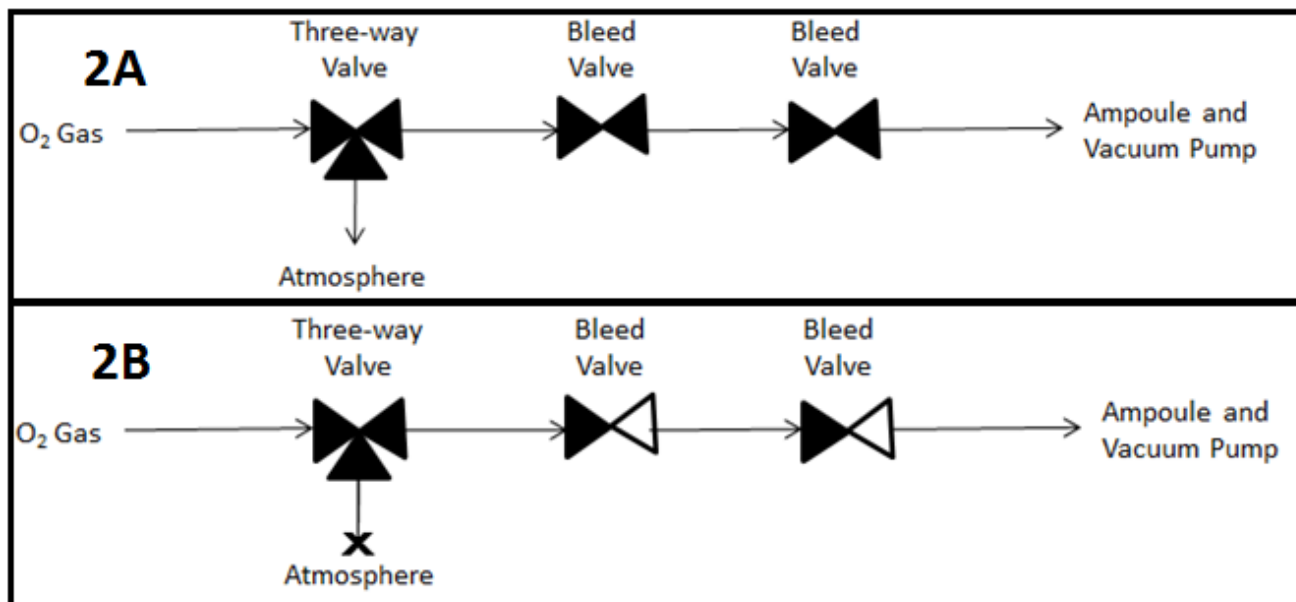


**Figure 2A:** First valve configuration. O<sub>2</sub> gas is flushing air out of system up to three-way valve. The vacuum pump is removing air up to the three-way valve, including both bleed valves. **Figure 2B:** Second valve configuration. O<sub>2</sub> gas is now free to flow through the three-way valve while the partially open bleed valves control the gas flow.

## 2.2 Slotted Ring Deflection Measurements

After completing a five-day heating regimen, the ring samples were cleaned and subjected to elastic loads to evaluate their mechanical resistance. The corresponding ring deflections were recorded using a deflection measurement apparatus developed by Quastelet *et al.* [12]. Equation 2 displays the expected deflection of a ring sample,  $D_y$ , when placed under a mass load ( $F_y = mg$ ) where  $R$  is the radius,  $l$  is the width,  $E$  is the Young's modulus, and  $t$  is the ring thickness.

$$D_y = \frac{36\pi R^3 F_y}{Elt^3} \quad (2)$$

Small changes in ring thickness can be measured because the deflection experienced by a ring is proportional to the inverse cube of its thickness (Equation 2). Thus, deflection measurements can be used to quantify the severity of corrosive attacks that actively reduce the sample thickness.

## 3. Results and Discussion

The following subsections outline results and statistical analyses intended to determine whether the presence of  $O_2$  gas,  $Na_2O$ , or  $CaO$  limit the increases in  $D_y$  (*e.g.*, reduction of ring thickness) caused by chemical reactions between iodine and Zr-4. Conclusions will be drawn by comparison of this work to a previously compiled baseline dataset collected by Metzler *et al.* [11].

### 3.1 Oxygen Gas Additions

Figure 3 displays the deflection ( $D_y$ ) results for a 95 g mass-load for 116 distinct ring samples. As listed in Table 1, ring samples were stressed on 6-12 mm wide Zr-4 wedges and heated at 300 °C or 375 °C. Based on the distribution of all results (Figure 3), one cannot readily determine if increasing the oxygen pressure significantly limits the extent of iodine attack. Therefore, to develop a more complete and quantifiable understanding of whether  $O_2$  gas, temperature, and wedge size affect deflection results, a multivariable linear regression was performed using Microsoft Excel<sup>TM</sup>. Results from the first regression (Table 2) include an intercept of 1.0, standard error of 0.12, and a  $p$ -value of  $4 \times 10^{-14}$ .

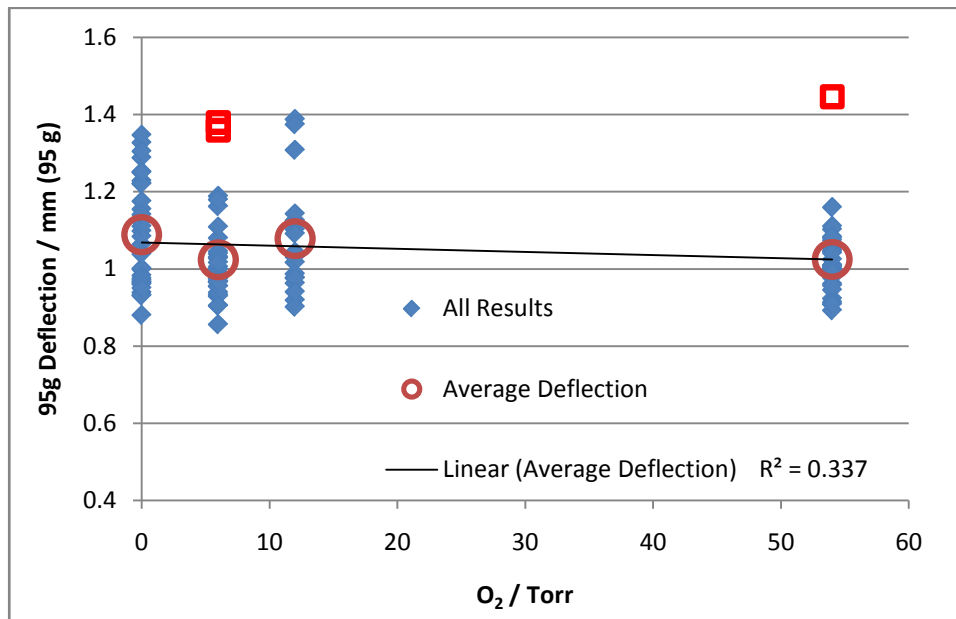


Figure 3: 95 g deflection results for all O<sub>2</sub> gas tests. Red squares denote outliers and red circles display the average deflection at each O<sub>2</sub> level (excluding outliers). The trend line and R<sup>2</sup> value are based on average deflection values for each O<sub>2</sub> gas level.

Table 2: Preliminary regression results for O<sub>2</sub> gas data set.

Parameter	Coefficients	Standard Error	<i>p</i> -value
Temperature	$3 \times 10^{-4}$	$3 \times 10^{-4}$	0.32
O <sub>2</sub> Gas	$-9 \times 10^{-4}$	$5 \times 10^{-4}$	0.09
Wedge Size	$-6 \times 10^{-3}$	$6 \times 10^{-3}$	0.30

The results in Table 2 are interpreted using the *p*-values, from which one can determine the confidence level for whether a parameter can be determined as a statistically significant factor. For a parameter to be accepted at the 95% confidence level, the *p*-value attached must be less than 0.05. From Table 2, it can be seen that both temperature and wedge size have not had a significant effect on deflections (*p*-value > 0.1) while the effect of oxygen gas is between the 95% and 90% confidence levels ( $0.05 < p\text{-value} < 0.1$ ). Backwards elimination regression analysis requires the least significant factor that has a *p*-value greater than 0.05 to be removed from the analysis and to re-run the regression as such [13]. Temperature and wedge size were sequentially removed from the regression analysis as temperature had the highest *p*-value from the initial regression, and a secondary regression featuring only O<sub>2</sub> gas and wedge size as parameters produced a *p*-value of 0.23 for wedge size. The final regression included an intercept of 1.07 with a standard error of 0.02 and a *p*-value of  $2 \times 10^{-95}$ . The final result for the O<sub>2</sub> gas parameter was a coefficient of  $-8 \times 10^{-4} \text{ torr}^{-1}$  with a standard error of  $5 \times 10^{-4}$  and a *p*-value of 0.13.

The *p*-value for O<sub>2</sub> gas is now outside of requirement for even a 90% confidence level (*p*-value > 0.1), which would not allow O<sub>2</sub> gas to be accepted as a statistically significant factor in terms of affecting deflection results. However, when inspecting the points in Figure 3, it can be seen that there are data points at each oxygen level that appear to be significantly higher than the rest of the data at said level of

O<sub>2</sub> gas. In light of this, an investigation was performed to try and determine if any of these data points could be classified as outliers and removed from the dataset.

### 3.1.1 Identification of statistical outliers

Tukey's method was used in an attempt to search for data points that could be classified as outliers [14]. The process of Tukey's method begins by determining the first ( $Q1$ ) and third quartile ( $Q3$ ) values in a dataset.  $Q1$  represents the point where 25% of the dataset occurs below this value, whilst  $Q3$  is the point where 25% of the dataset occurs above this value. For this investigation, built-in Microsoft Excel<sup>TM</sup> functions were used to determine  $Q1$  and  $Q3$  for each level of O<sub>2</sub> gas addition. The interquartile range,  $IQR$ , could then be determined using  $Q1$  and  $Q3$  as shown in Equation 3.

$$IQR = Q3 - Q1 \quad (3)$$

The upper and lower fences values were then determined using Equations 4 and 5.

$$Lower\ Fence = Q1 - (IQR * 3) \quad (4)$$

$$Upper\ Fence = Q3 + (IQR * 3) \quad (5)$$

Results that fall outside of the range set by the lower and upper fence can be categorized as outliers. It should be noted that the value used to multiply the  $IQR$  by is often 1.5 instead of 3. For this analysis, a higher value was selected to provide a more conservative approach in determining outliers. This approach was selected because the experimental method used in this paper yielded high variance results and a less conservative approach would suggest that a large amount of data should be removed. The conservative approach led to the removal of three data points: two points from the 6 Torr results; and one point from the 54 Torr results (depicted by red squares in Figure 3). It is unclear what caused these outliers to occur as each result came from separate tests where a single ring displayed significantly higher deflection from the other results. It appears as though wedge size does not play a role in producing results classified as outliers, as the outliers came from results on wedges of different sizes. It also seems unlikely that a specific ring would display higher deflection due to increased iodine exposure, as the iodine present surely sublimated into a gas that would spread evenly throughout the ampoule. It is possible that these high deflection rings received a higher strain level when being loaded onto the static wedge or featured a small mechanical defect that led to increased deflection.

### 3.1.2 Regression with outliers excluded

After the outliers were excluded, a regression analysis performed on the revised dataset indicates that our confidence in the existence of a linear relationship between O<sub>2</sub> gas pressure and deflection improved (*i.e.*, the  $p$ -value decreased from 0.13 to 0.06). The regression includes an intercept of 1.1 with a standard error of 0.01 and a  $p$ -value of  $9 \times 10^{-98}$ . The result for the O<sub>2</sub> gas parameter was a coefficient of  $-9 \times 10^{-4} \text{ torr}^{-1}$  with a standard error of  $4 \times 10^{-4}$  and a  $p$ -value of 0.06.

Thus, with outliers excluded, O<sub>2</sub> gas could be accepted as a statistically significant factor at the 90% confidence level, but not at the 95% confidence level. At an O<sub>2</sub> level of 54 Torr, the regression would predict the deflection to decrease by  $0.05 \pm 0.02$  mm. This indicates that, according to regression analysis, it can be said with 90% confidence that the inclusion of O<sub>2</sub> gas has produced a low level of SCC mitigation.

### 3.1.3 Comparison with previous work

Although the relationship between O<sub>2</sub> gas pressure and mechanical deflection is not an obviously linear one, previous work suggests that the relationship should not be linear. For example, Uneet *al.* found that SCC mitigation occurred in Zircaloy-2 (Zr-2) when the oxygen pressure exceeded a threshold value (*i.e.*, 28 Torr at 300 °C), and that increasing the oxygen gas pressure above the threshold led only to marginal improvements [15]. Evidence of SCC mitigation has also been observed in Zircaloy-4 when the O<sub>2</sub> gas pressure reached a threshold pressure (approximately 11.75 Torr at 300 °C) above, albeit for small sample sizes [12]. The differences in the O<sub>2</sub> pressure thresholds seen by Uneet *al.* and what was seen in this paper may arise from the fact that the experiments of Uneet *al.* investigated the time required for Zr-2 to reach the failure regime, while this paper analysed pre-failure corrosion levels in Zr-4 samples.

Close inspection of Figure 3 (with outliers removed) reveals that a relationship may exist whereby a threshold oxygen pressure is reached and limited improvements in deflection are observed above the threshold pressure. For instance, if the deflections corresponding to 6, 12, and 54 Torr (all pressures at room temperature) are not distinct from one another, yet significantly lower than the deflection corresponding to the baseline condition (0 Torr added), then the non-linear trend can be characterized by a plateau region covering all pressures above a threshold pressure of 6 Torr (approximately 11.75 Torr at 300 °C).

To determine quantitatively whether this trend is occurring, a *two-tailed*, type three *t*-test was performed. Oxygen data was split into two arrays: deflection results where O<sub>2</sub> gas was introduced and deflection results where O<sub>2</sub> gas was not introduced (baseline results). The *t*-test returned a result of 0.0165; meaning that it can be stated at the 95% confidence level that results with elevated O<sub>2</sub> gas were statistically distinct from the baseline results. The reason that the *t*-test produced a higher confidence level than the regression results lies within the fact that regression analysis presupposes a linear relationship across two variables. If these data were truly experiencing a plateau after the first point there would be no linear relationship to be found across the three levels of O<sub>2</sub> gas tested. This would lead to a low R<sup>2</sup> value (Figure 3) and a low *p*-value (Table 2). The *t*-test analysis, however, simply states the likelihood that two datasets are distinct and thusly was able to provide an understanding at a higher confidence level. This analysis indicates that Figure 3 likely illustrates a non-linear relationship between O<sub>2</sub> gas pressure and mechanical deflection characterized by a plateau region covering all pressures above a threshold pressure of 6 Torr (approximately 11.75 Torr at 300 °C).

## 3.2 Na<sub>2</sub>O and CaO Additions

The dataset used for the metal oxide additive investigation is comprised of 144 slotted rings that were placed on static wedges of various sizes in a hot (300 °C) and corrosive (1530 mg of I<sub>2</sub>) environment for five days with varied amounts of CaO and Na<sub>2</sub>O.

Regression analysis was performed to model the deflections experienced by each ring when loaded with 95 g. The parameters included are: mass of Na<sub>2</sub>O powder, mass of CaO powder, and wedge size. Since temperature and iodine concentration remained the same in all experiments, these factors were not included as parameters in the regression analysis. The results for each parameter from the preliminary regression results are shown in Table 3. The regression model produced an intercept value of 1.11, a standard error of 0.03, and a *p*-value of  $3.4 \times 10^{-76}$ .

**Table 3: Initial regression results for metal oxide additive experiments.**

Parameter	Coefficients	Standard Error	<i>p</i> -value
Na <sub>2</sub> O (g)	-0.22	0.03	$2 \times 10^{-12}$
CaO (g)	-0.82	0.06	$7 \times 10^{-26}$
Wedge Size (mm)	$1 \times 10^{-3}$	$3 \times 10^{-3}$	0.69

Negative coefficients and low *p*-values (<0.05) in Table 3 indicate that increasing amounts of Na<sub>2</sub>O or CaO mass will lead to a statistically significant decrease in the slotted ring deflection induced by a 95 g mass load. Conversely, the large *p*-value (> 0.05) for wedge size once again indicates that the value of wedge size (*i.e.* induced stress) does not display a correlation with 95g induced ring deflection. However, as these oxides have different molar masses (Na<sub>2</sub>O =  $62 \text{ g mol}^{-1}$  and CaO =  $56 \text{ g mol}^{-1}$ ) it is difficult to compare the relative impact of these oxides on ring deflection purely based on mass (where the coefficient unit is  $\text{mm g}^{-1}$ ). Therefore, the regression was modified to determine the deflection decreases resulting from one mole of each oxide. The mass values are converted into moles using Equations 6 and 7:

$$n_{Na_2O} = \frac{m_{Na_2O}}{M_{Na_2O}} \quad (6)$$

$$n_{CaO} = \frac{m_{CaO}}{M_{CaO}} \quad (7)$$

Where *n* is moles, *m* is mass, and *M* is molar mass. This conversion allows for one to compare the magnitude of the decrease in deflection caused by both of the oxides across a neutral plane of moles. The results from an updated regression using mole values (with a y-intercept value of 1.06, a standard error of 0.02, and a *p*-value of  $4.14 \times 10^{-81}$ ) are shown below in Table 4.

**Table 4: Regression results using moles of alkaline oxide as input**

Parameter	Coefficients (mm mole <sup>-1</sup> )	Standard Error	<i>p</i> -value
Na <sub>2</sub> O	-14	2	$2 \times 10^{-12}$
CaO	-46	4	$4 \times 10^{-26}$

It can be seen that both of the *p*-values are quite low, suggesting that the effect of both oxides have remained statistically significant. In addition, with the units of the input converted to moles, it is

possible to compare the effect of the oxides on a more neutral basis (*e.g.*, moles of oxide). From this analysis it can be stated that the negative slope in deflection results from including small amounts of CaO is approximately three times more negative than the slope seen from including small amounts of Na<sub>2</sub>O. It should be noted that the regression analysis used to perform this investigation presupposes that the factors being analyzed follow a linear trend. Figures 4 and 5 display the results from the experiments in an attempt to determine whether the assumption of linearity holds true for the dataset.

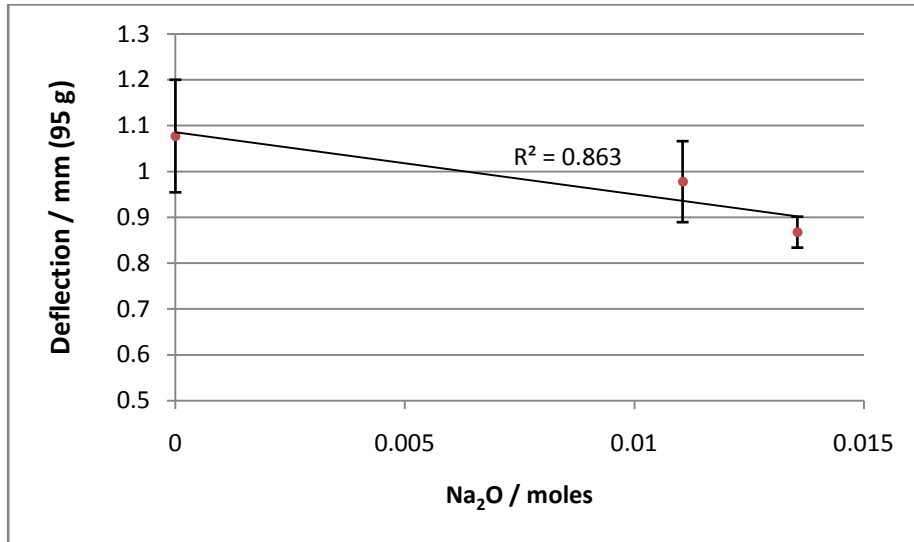


Figure 4: Average Na<sub>2</sub>O deflection results (error bars = 1  $\sigma$ ).

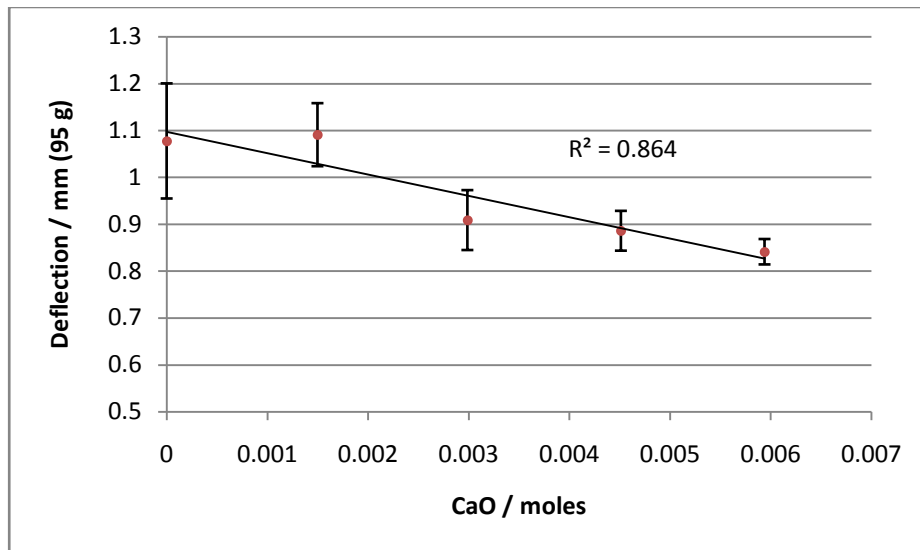


Figure 5: Average CaO deflection results (error bars = 1  $\sigma$ ).

Although the Na<sub>2</sub>O trend line correlates well with the experimental data ( $R^2 > 0.85$ ), having only three  $x$ -values is likely insufficient to conclusively state a linear relationship (Figure 4). Consequently, experimental efforts were undertaken to include varying levels of CaO in order to clarify whether the correlation between oxide levels and deflection is linear. CaO was selected as the oxide to be characterized further after initial CaO deflection results were lower than initial Na<sub>2</sub>O results. In Figure 5 there is a reasonably strong negative linear correlation ( $R^2 > 0.85$ ) seen in the range of CaO

results displayed, which features a more varied set of oxide levels. It should be noted that the second point, occurring at ~0.0015 moles of CaO, Figure 5, is essentially the same as the first point where results were collected without CaO. It remains unknown whether this is an actual plateau where SCC mitigation only occurs after a certain threshold, or if there simply was such a small amount of oxide present that it proves difficult to discern the effect of the CaO with the amount of error present in the measurements. Although the current results are preliminary, the decreasing trend in ring deflection suggests that these oxides may assist in SCC mitigation.

#### 4. Conclusion

In conclusion, a series of tests were performed to investigate the influence of O<sub>2</sub> gas, Na<sub>2</sub>O, and CaO on iodine-induced stress corrosion cracking in CANDU Zr-4 fuel sheathing. Results were analysed using deflection measurements, which can reflect small changes in ring thickness. Regression analysis performed on O<sub>2</sub> gas data was not conclusive in showing a negative linear trend in deflection (*i.e.*, improved performance) as the amount of O<sub>2</sub> gas increased, even after statistical outliers had been removed. However, when the baseline dataset (no additional O<sub>2</sub> exposure) was compared with a dataset containing all O<sub>2</sub>-exposed rings (6-54 Torr) a *t*-test revealed that O<sub>2</sub> gas created a statistically distinct dataset at the 95% confidence level. This suggests that the presence of O<sub>2</sub> gas improves the resistance of Zr-4 to iodine-induced corrosion to a certain level. For Zr-4, this improvement in deflection occurred at a threshold oxygen pressure of 6 Torr or less (at room temperature) and led to a decrease in average deflection from 1.09 mm to 1.02 mm. This provides an understanding of the magnitude of the decrease in deflection that can be expected when at least  $1 \mu\text{mol}_{\text{O}_2} \text{cm}^{-2}_{\text{Zr-4}}$  is present.

A regression analysis of the metal oxide results determined that increasing the quantities of CaO and Na<sub>2</sub>O significantly decreased the corresponding ring deflections. The regression analysis indicates that additions of CaO decrease deflection at a steeper rate than Na<sub>2</sub>O. Experiments without any oxide additives had an average deflection of  $1.1 \pm 0.1$  mm. When the highest concentration of Na<sub>2</sub>O was introduced the average deflection decreased to  $0.86 \pm 0.03$  mm. When the highest concentration of CaO was introduced the average deflection decreased to  $0.84 \pm 0.03$  mm. Based on deflection data collected at five molar quantities of CaO, it was determined there's a linear trend between CaO additions and mechanical deflection. Additional metal oxides, such as magnesium oxide (MgO), may now be investigated with an understanding that increasing amounts of oxide will most likely display a negative linear correlation in deflection results. The experimental evidence presented here indicates that Na<sub>2</sub>O and CaO, which are naturally available as impurities in CANLUB, potentially play an important role in limiting iodine-induced stress corrosion cracking. As such, further investigation into introducing higher amounts of these oxides into CANDU reactors through the doping of CANLUB may be warranted.

#### 5. Acknowledgments

The authors acknowledge the financial support of Natural Sciences and Engineering Research Council of Canada, the CANDU Owners' Group, and University Network of Excellence in Nuclear Engineering for financial support of this research. The authors are appreciative of the technical expertise and guidance of Tim Nash and Clarence McEwen, as well as Aaron Quastel, whose work formed the basis of the experiments performed in this paper.

## 6. References

---

- [1] R. Cottis, “Guides To Good Practice In Corrosion Control - Stress Corrosion Cracking”, *National Physical Laboratory*, 2000.
- [2] B.J. Lewis, W.T. Thompson, M.R. Kleczek, K. Shaheen, M. Juhas, and F.C. Iglesias, “Modelling Of Iodine-Induced Stress Corrosion Cracking In Candu Fuel,” *Journal of Nuclear Materials*, vol. 408, pp. 209-223, 2011.
- [3] P. Sidky, “Iodine Stress Corrosion Cracking Of Zircaloy Reactor Cladding: Iodine Chemistry (A Review),” *Journal of Nuclear Materials*, vol. 256, pp. 1-17, 1998.
- [4] B. Cox and J.C. Wood, “Iodine Induced Cracking of Zircaloy Fuel Cladding- A Review,” *Atomic Energy of Canada Limited*, 1974.
- [6] J.A. Robertson, R.D. Page, and L.L. Bodie, “Canadian Fuel Performance,” in ANS Annual Meeting, Chicago, Illinois, AECL-4520, 1973.
- [7] P.K. Chan and K.J. Kaddatz, “How Does CANLUB Work,” in 15<sup>th</sup> Annual Conference of the Canadian Nuclear Association, Toronto, 1994.
- [8] J.C. Wood, B.A. Surette, I. Atchison, and W.R. Clendening, “Pellet Cladding Interaction - Evaluation of Lubrication by Graphite,” *Journal of Nuclear Materials*, vol. 88, pp. 81-94, 1980.
- [9] M.R. Kleczek, K. Shaheen, W.T. Thompson, B.J. Lewis, and F.C. Iglesias, “Iodine Stress Corrosion Cracking and Possible Mitigation Strategy for CANDU fuel,” in 11<sup>th</sup> International Conference on CANDU Fuel, Kingston, Canada, 2010.
- [10] J. Wood, “Factors Affecting Stress Corrosion Cracking Of Zircaloy In Iodine Vapour,” *Journal of Nuclear Materials*, vol. 45, pp. 105-122, 1972.
- [11] J. Metzler, G.A. Ferrier, M. Farahani, P.K. Chan, and E.C. Corcoran, “An Analysis of Static Loading Results on Slotted Ring Samples to Allow for Further Investigation of Stress Corrosion Cracking,” in 2014 Pacific Basin Nuclear Conference, Vancouver, Canada, 2014.
- [12] A.D. Quastel, E.C. Corcoran, and B.J. Lewis, “The Effect Of Oxidized U<sub>2</sub>O On Iodine-Induced Stress Corrosion Cracking Of Fuel Sheathing,” in 12<sup>th</sup> International Conference on CANDU Fuel, Kingston, Canada, 2013.
- [13] M.A. Efron, (1960) “Multiple Regression Analysis.” In Ralston, A. and Wilf, HS, editors, *Mathematical Methods for Digital Computers*. Wiley.
- [14] J.W. Tukey, (1977). *Exploratory Data Analysis*. Addison-Wesley.
- [15] K. Une, “Stress Corrosion Cracking of Zircaloy-2 Cladding in Iodine Vapor,” *Journal of Nuclear Science and Technology*, vol. 14, pp. 443-451, 1977.